

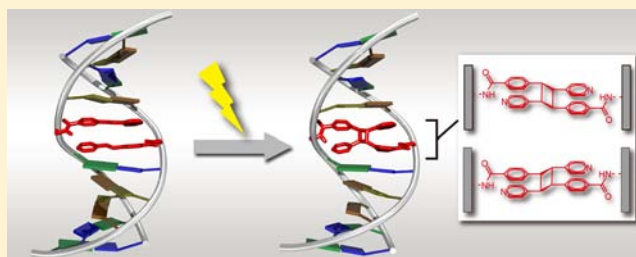
p-Stilbazole Moieties As Artificial Base Pairs for Photo-Cross-Linking of DNA Duplex

Hiromu Kashida,* Tetsuya Doi, Takumi Sakakibara, Takamitsu Hayashi, and Hiroyuki Asanuma*

Graduate School of Engineering, Nagoya University, Furo-cho, Chikusa-ku, Nagoya 464-8603, Japan

S Supporting Information

ABSTRACT: In this study, we report a photo-cross-linking reaction between *p*-stilbazole moieties. *p*-Stilbazoles were introduced into base-pairing positions of complementary DNA strands. The [2 + 2] photocycloaddition reaction occurred rapidly upon light irradiation at 340 nm. Consequently, duplex was cross-linked and highly stabilized after 3 min irradiation. The CD spectrum of the cross-linked duplex indicated that the B-form double-helical structure was not severely distorted. NMR analysis revealed only one conformation of the duplex prior to UV irradiation, whereas two diastereomers were detected after the photo-cross-linking reaction. Before UV irradiation, *p*-stilbazole can adopt two different stacking modes because of rotation around the single bond between the phenyl and vinyl groups; these conformations cannot be discriminated on the NMR time scale due to rapid interconversion. However, photo-cross-linking fixed the conformation and enabled discrimination both by NMR and HPLC. The artificial base pair of *p*-methylstilbazolium showed almost the same reactivity as *p*-stilbazole, indicating that positive charge does not affect the reactivity. When a natural nucleobase was present in the complementary strand opposite *p*-stilbazole, the duplex was significantly destabilized relative to the duplex with paired *p*-stilbazole moieties and no photoreaction occurred between *p*-stilbazole and the nucleobase. The *p*-stilbazole pair has potential as a “third base pair” for nanomaterials due to its high stability and superb orthogonality.



INTRODUCTION

Watson–Crick base pairs stabilize DNA duplexes through hydrogen-bonding and stacking interactions. Extremely high orthogonality of base pairing is realized by strict control of these two interactions. It has become possible to synthesize oligodeoxyribonucleotides of essentially any sequence in an automated fashion. This has made DNA an ideal material to construct nanostructures and nanodevices.^{1,2} DNA duplexes dissociate into single strands at high temperature. Although the reversibility is essential for biological processes, such as replication and transcription, the heat lability of DNA duplex in some cases restricts applications of DNA-based nanomaterials. To make DNA nanomaterials more heat tolerant, it is necessary to increase the thermal stability of DNA structures.³

Photo-cross-linking or photoligation has been widely studied not only for its biological relevance but also for nucleic acid detection and duplex stabilization.^{4–7} For example, Lewis et al. reported photo-cross-linking system by introducing stilbene units into main chain of a DNA duplex.⁸ Fujimoto et al. reported several vinyldeoxyuridine and vinylcarbazole derivatives that form adducts with natural nucleobases.⁹ Cross-linking has been used in SNP detection, DNA computing, and nanostructure stabilization.^{10–14} Furthermore, photoligation via [4 + 4] cycloaddition reaction between anthracene moieties has been reported by Ihara et al. and other groups.^{15–18}

Herein, we propose a photo-cross-linking system using *p*-stilbazoles as an artificial base pair. We have previously reported

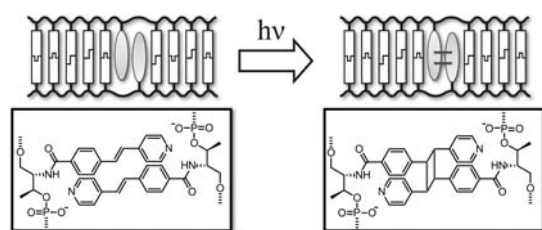
that planar molecules incorporated via D-threoninol linkers serve as “artificial base pairs” to stabilize a DNA duplex.¹⁹ For example, when azobenzene derivatives were introduced into the base-pairing positions of both strands, the duplex was highly stabilized relative to the unmodified DNA due to intermolecular stacking interactions.^{20,21} Interestingly, this “base pair” showed high orthogonality with natural base pairs. We have also reported that base pairs of *p*-methylstilbazolium, which has a positive charge, stabilize duplexes even more strongly than natural base pairs due to electrostatic interactions between the positive charge on *p*-methylstilbazolium and the phosphate anion.^{22,23} In this paper, we used the photocycloaddition reaction between stilbazole derivatives to further improve the heat tolerance of a DNA duplex.

p-Stilbazole derivatives are known to form dimers upon UV irradiation via a [2 + 2] photocycloaddition reaction.^{24–26} Therefore, if a duplex containing an artificial base pair of *p*-stilbazole moieties is irradiated with UV light, the *p*-stilbazoles should react with each other and the duplex should be cross-linked (Scheme 1). If the *p*-stilbazole base pair shows high orthogonality, *p*-stilbazoles could serve as a “third base pair” for preparation of complex nanomaterials. Here, we introduced *p*-stilbazole moieties (**B** in Figure 1) into DNA and investigated their photoreactivity and effect on duplex stability. *p*-

Received: February 20, 2013

Published: May 3, 2013

Scheme 1. Schematic Illustration of Photo-Cross-Linking via [2 + 2] Photocycloaddition Between *p*-Stilbazole Moieties



Xa: 5'-GCATCXAGTC-3' (X=A, T, G, C, B, Z)
Xb: 3'-CGTAGXTCAg-5' (X=A, T, G, C, B, Z)
N: 3'-CGTAGTCAG-5'

Bc: 5'-GGABGTC-3'
Bd: 3'-CCTBCAG-5'

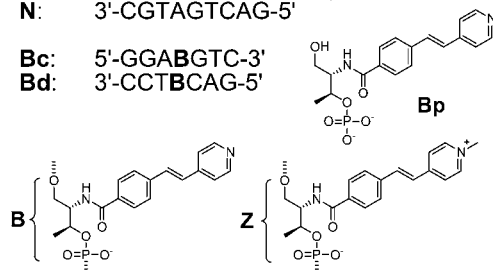


Figure 1. Sequences of ODNs synthesized in this study. Chemical structure of *p*-stilbazole monophosphate is also shown.

Methylstilbazolium (Z in Figure 1), which has a similar structure but a positive charge, was also incorporated into DNA to investigate the effects of positive charge on photoreactivity. Orthogonality of stilbazole moieties with natural base pairs was also evaluated.

EXPERIMENTAL SECTION

Materials. All the conventional phosphoramidite monomers, CPG columns, and reagents for DNA synthesis were purchased from Glen Research. Other reagents for the synthesis of phosphoramidite monomers were purchased from Tokyo Chemical Industry, Wako, and Aldrich. Unmodified oligodeoxyribonucleotides (ODNs) were purchased from Integrated DNA Technologies.

Synthesis of ODNs. All modified ODNs were synthesized on an automated DNA synthesizer (H-8-SE, Gene World) by using phosphoramidite monomers bearing B or Z. Syntheses of phosphoramidite monomers B and Z were reported previously.²² *p*-Stilbazole monophosphate was synthesized as described in the Supporting Information. Sample handling was conducted under dark conditions. After the workup, ODNs were purified by reversed phase HPLC and characterized using a MALDI-TOF MS (Autoflex II, Bruker Daltonics). Matrix-assisted laser desorption ionization time-of-flight mass spectrometry (MALDI-TOF MS) data for the synthesized ODNs: **Ba**: obsd 3072 (calcd for [**Ba** + H⁺]: 3073). **Bb**: obsd 3112 (calcd for [**Bb** + H⁺]: 3113). **Bc**: obsd 2206 (calcd for [**Bc** + H⁺]: 2206). **Bd**: obsd 2126 (calcd for [**Bd** + H⁺]: 2126). **Za**: obsd 3088 (calcd for [**Za** + H⁺]: 3088). **Zb**: obsd 3128 (calcd for [**Zb** + H⁺]: 3128).

NMR Measurements. NMR samples were prepared by dissolving lyophilized DNA in an H₂O/D₂O 9:1 solution containing 10 mM sodium phosphate (pH 7.0) to give a duplex concentration of 1.0 mM. NaCl was added to give a final sodium concentration of 200 mM. NMR spectra were measured with a Varian INOVA spectrometer (700 MHz) equipped for triple resonance at a probe temperature of 275 K. Resonances were assigned by standard methods using a combination of 1D, totally correlated spectroscopy (TOCSY) (60 ms of mixing time), and nuclear Overhauser effect spectroscopy (NOESY) (150 ms of mixing time) experiments. All spectra in the H₂O/D₂O 9:1 solution were recorded using the 3–9–19 WATERGATE pulse sequence for water suppression.²⁷

Spectroscopic Measurements. UV spectra were measured on a JASCO model J-560 equipped with a programmed temperature controller; 10 mm quartz cells were used. CD spectra were measured on a JASCO model J-820 equipped with programmed temperature controllers using 10 mm quartz cells.

Measurement of the Melting Temperature. The melting curves were obtained with a JASCO model J-560 by measuring the change in absorbance at 260 nm versus temperature. The melting temperature (T_m) was determined from the maximum in the first derivative of the melting curve. Both the heating and the cooling curves were measured, and the calculated T_m s agreed to within 2.0 °C. The temperature ramp was 1.0 °C min⁻¹.

UV Irradiation. A xenon light source (MAX-301, Asahi Spectra) equipped with interference filters centered at 341.5 nm (half bandwidth 9 nm, power density 0.15 mW/cm²) was used for photo-cross-linking. The sample solution was added to a cuvette, and the temperature of light irradiation was controlled using a programmable temperature controller. Photoirradiation was conducted at 0 °C.

HPLC Analyses. A Merck LiChrospher 100 RP-18(e) column heated at 50 °C was used for HPLC analyses. The flow rate was 0.5 mL/min. A solution of 50 mM ammonium formate (solution A) and a mixture of 50 mM ammonium formate and acetonitrile (50/50, v/v) (solution B) were used as mobile phases. A linear gradient of 5–35% solution B over 30 min was employed. HPLC chromatograms were monitored at 260 nm absorption.

Molecular Dynamic Simulation. The Insight II/Discover 98.0 program package was used for conformational energy minimization. The duplex tethering *p*-stilbazole was built from canonical B-form DNA by a graphical program. The AMBER95 force field was used for the calculation. All the structures were energy minimized to an RMS derivative of <0.001 kcal Å⁻¹. Computations were carried out on a Silicon Graphics O2+ workstation with the IRIX64 OS release 6.5.

RESULTS AND DISCUSSION

Photochemical Properties of *p*-Stilbazole Monophosphate and *p*-Stilbazole-Modified DNA. We first investigated the photochemical properties of *p*-stilbazole monophosphate (**Bp** in Figure 1) before evaluating photochemical properties in DNA. Figure 2a shows the UV–vis spectra of **Bp**

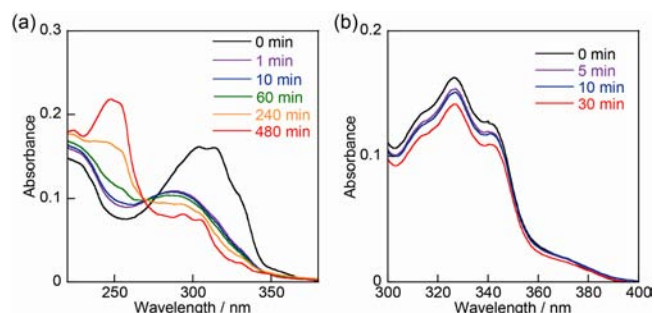
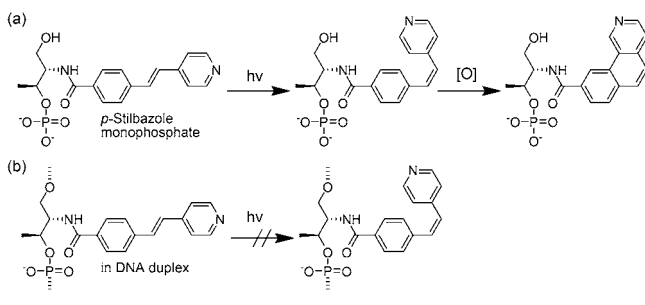


Figure 2. UV–vis spectra of (a) stilbazole monophosphate **Bp** and (b) **Ba/N** before and after UV irradiation (340 nm). T_m of **Ba/N** was 43.2 °C. Solution conditions were 5.0 μM **Bp**, 5.0 μM DNA, 100 mM NaCl, 10 mM phosphate buffer (pH 7.0), 0 °C.

before and after photoirradiation. Before photoirradiation, **Bp** showed peaks at 303 and 312 nm arising from the $\pi\pi^*$ transition of *trans* *p*-stilbazole (black line). When the sample was irradiated with 340 nm UV light for 1 min, these peaks immediately disappeared, and a new broad peak appeared at 297 nm due to photoisomerization to the *cis* form (purple line).²⁸ Thus, the photoisomerization rate of free *p*-stilbazole is intrinsically very rapid. Further photoirradiation at 340 nm for 480 min resulted in a decrease in absorbance at around 300 nm and appearance of a peak at 247 nm (red line). These spectral

shifts are due to cyclization and subsequent oxidation to a benzoquinoline derivative as shown in Scheme 2a.²⁹ The

Scheme 2. Photochemical Reaction Observed with (a) *p*-Stilbazole Monophosphate and (b) *p*-Stilbazole Moiety in DNA Duplex



cyclized product was detected by ESI-MS (see Supporting Information). The peak at around 300 nm did not disappear even after 480 min irradiation, indicating that the [2 + 2] photocycloaddition reaction did not occur under these conditions. These results show that photoirradiation of *p*-stilbazole potentially causes several side reactions but not the desired [2 + 2] photocycloaddition (Scheme 2a).

In striking contrast, incorporation of *p*-stilbazole into DNA drastically suppressed these side reactions. The **Ba**/N duplex with a stilbazole moiety in one strand of the DNA duplex showed absorption maximum (λ_{max}) at 327 nm (black line in Figure 2b). The peak did not change after irradiation at 340 nm for 5 min. Although the peak slightly decreased after 30 min irradiation, these results clearly demonstrated that introduction of *p*-stilbazole moiety into DNA strongly suppressed photoisomerization to *cis* form (Scheme 2b). This is in sharp contrast to azobenzene, which can isomerize even within DNA duplex.³⁰ This difference in isomerization is attributable to differences in the isomerization mechanisms: Isomerization of the stilbene derivative proceeds exclusively through rotation, whereas that of azobenzene occurs via both rotation and inversion.³¹ Consistently, photoisomerization of stilbene derivatives is suppressed in viscous solution, whereas isomerization of azobenzene is not affected significantly by viscosity.³² Within a DNA duplex, isomerization of *p*-stilbazole is presumably suppressed by stacking interactions with natural base pairs.

Photo-Cross-Linking of *p*-Stilbazole in DNA Duplex.

The photochemical properties of the duplex **Ba**/**Bb**, which has **B** residues in complementary positions on the two strands, were investigated in order to evaluate the photo-cross-linking of *p*-stilbazole within a duplex.³³ Before photoirradiation, the UV-vis spectrum of the **Ba**/**Bb** duplex had a peak at 323 nm (Figure 3). A slight hypsochromic shift compared with the single-stranded **Ba** (λ_{max} 325 nm) indicated that **B** residues formed an H dimer (Figure S1).³⁴ Upon irradiation at 340 nm for 3 min, the peak at 323 nm had completely disappeared. This disappearance of the π - π^* absorption band assigned to the *p*-stilbazole moieties strongly suggested that a [2 + 2] photocycloaddition reaction between two *p*-stilbazole moieties had occurred. The λ_{max} of **Ba**/**Bb** did not shift upon photoirradiation, indicating that *trans*-to-*cis* isomerization did not occur and that neither *p*-stilbazoles were in the *cis* form. Instead, the *trans* forms reacted. Note that isomerization to the *cis* form causes a blue-shift in the absorption spectrum as shown in Figure 2A.

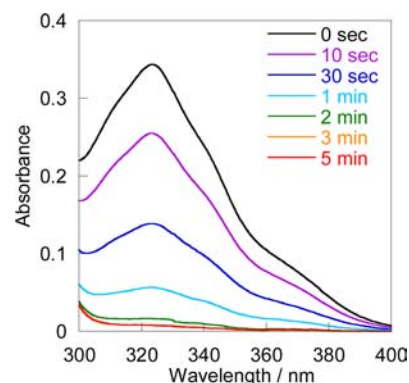


Figure 3. UV-vis spectra of **Ba**/**Bb** before and after photoirradiation. Solution conditions were 5.0 μM DNA, 100 mM NaCl, 10 mM phosphate buffer (pH 7.0), 0 $^{\circ}\text{C}$.

The photo-cross-linked product of **Ba**/**Bb** was further analyzed by reversed-phase HPLC (Figure 4). Before photo-

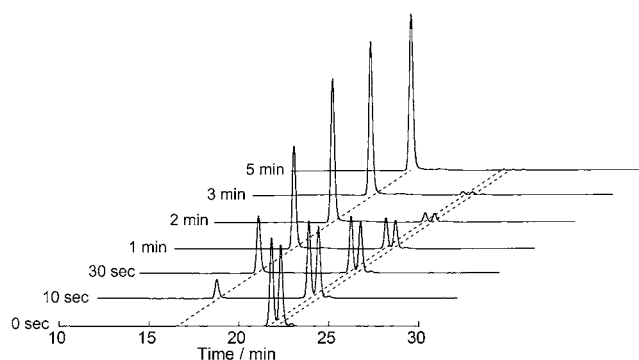


Figure 4. HPLC chromatograms of **Ba**/**Bb** before and after indicated times of photoirradiation.

irradiation, two peaks corresponding to the single-stranded forms of **Ba** and **Bb** were observed. After 3 min photoirradiation, however, the two peaks disappeared and a new peak appeared at a shorter retention time. MALDI-TOF MS analysis of this new peak proved it to be a photo-cross-linked duplex (Figure S2). From these results, we conclude that a [2 + 2] photocycloaddition reaction occurred between *p*-stilbazole moieties in the DNA duplex upon UV irradiation at 340 nm.

Structure of Photodimer of *p*-stilbazole. Photocycloaddition of stilbene derivatives usually produces several isomers.²⁴ When the stilbene derivatives are within a DNA scaffold, the orientations of *p*-stilbazoles should be restricted, and thus the stereochemistry of photodimerized product should be controlled. In order to investigate the structure of photo-cross-linked product, the **Bc**/**Bd** duplex was analyzed by NMR. The imino region of the 1D spectrum of **Bc**/**Bd** had six peaks corresponding to imino protons from the six natural base pairs (Figure 5a). These sharp peaks indicated that hydrogen bonding of natural base pairs was not disturbed by the presence of the *p*-stilbazole moieties. After irradiation at 340 nm, these peaks disappeared, and eight new peaks appeared. Although several peaks overlap, the appearance of more than six peaks indicates that there are at least two species in the photo-cross-linked product.

The aromatic regions of the 1D NMR spectra in D_2O of **Bc**/**Bd** before and after irradiation are shown in Figure 5b. In the nonirradiated sample, 11 peaks corresponded to 4 vinyl and 8

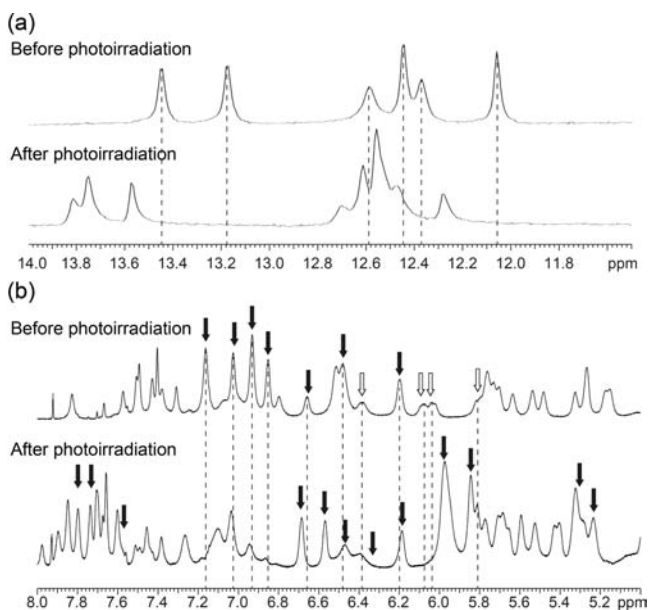


Figure 5. ^1H NMR spectra of **Bc/Bd** in (a) imino regions measured in $\text{H}_2\text{O}/\text{D}_2\text{O}$ and (b) aromatic regions in D_2O . White and black arrows in (b) indicate vinyl and phenyl protons of the *p*-stilbazole moiety, respectively.

phenyl protons of 2 *p*-stilbazole moieties.³⁵ In the spectrum of the irradiated sample, 4 peaks assigned to vinyl protons disappeared as expected, and 12 new, partially overlapping peaks appeared. If the photo-cross-linked product were a single species, only eight peaks should be observed. Hence, the appearance of 12 peaks clearly shows that more than one species was produced upon photoirradiation. Furthermore, TOCSY in D_2O gave eight cross-peaks in the aromatic region after photoirradiation, whereas four cross-peaks were observed before photoirradiation (Figure S3). These results undoubtedly show that there are two diastereomers of the photo-cross-linked product. The existence of two diastereomers was further supported by the appearance of two peaks in the HPLC chromatogram of **Bc/Bd** after irradiation (Figure S4).³⁶

Previously, we prepared DNA duplexes containing heterodimers of azo compounds. NMR structural analyses revealed that the dyes were stacked in an antiparallel manner and located at 3' side of the complementary strand.²¹ Thus, *p*-stilbazole moieties in this study are expected to adopt similar stacking structures. A *trans*-to-*cis* isomerization within the duplex could be ruled out based on the fact that the λ_{max} of **Ba/Bb** did not shift during photoirradiation (Figure 3). Furthermore, NMR and HPLC analyses revealed that equal amounts of diastereomers were produced. Thus, we concluded that the two observed products are diastereomers (Figure 6, right panel). The very fast rotation around the single bond between phenyl and vinyl groups of *p*-stilbazole results in the production of the two diastereomers upon irradiation. Before photoirradiation, *p*-stilbazole can adopt either of two stable stacking modes (Figure 6, left panel). Since interconversion between the two conformers is rapid, NMR does not distinguish these two conformers. Photo-cross-linking prevents interconversion and fixes the conformation. As a result, duplexes containing each of these two "fixed" conformers are observed both by NMR and HPLC. We have also conducted molecular dynamics simulations of **Ba/Bb** (Figure S5). These simulations indicate

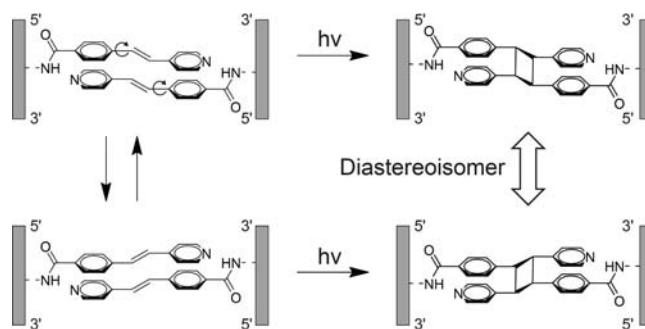


Figure 6. Presumed structures of diastereomers produced upon photocycloaddition.

that the *p*-stilbazoles in **Ba/Bb** may adopt either of the possible conformations without disturbing the overall B-form structure.

Thermal Stability of Photo-Cross-Linked Duplex. We next evaluated thermal stability of the cross-linked duplex. Melting curves of **Ba/Bb** before and after photoirradiation are shown in Figure 7a. Before photoirradiation, the T_m of **Ba/Bb**

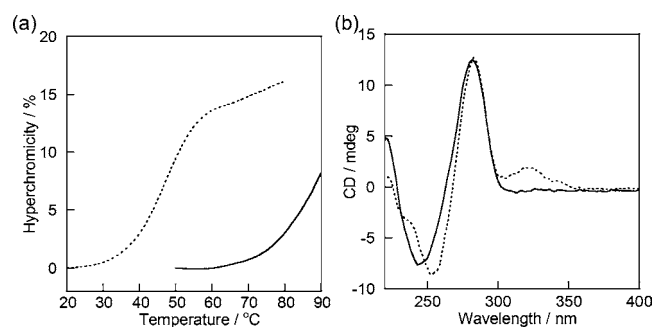


Figure 7. (a) Melting curves and (b) CD spectra of **Ba/Bb** before (dotted line) and after photoirradiation (solid line). Solution conditions were 5.0 μM DNA, 100 mM NaCl, 10 mM phosphate buffer (pH 7.0), 0 $^\circ\text{C}$.

Table 1. Comparison of Thermal Stabilities and Photoreactivities of Duplexes Containing *p*-Stilbazole and *p*-Methylstilbazolium

sequence	$T_m/^\circ\text{C}^a$		$k_{\text{obs}}/\text{min}^{-1c}$
	before UV irradiation	after UV irradiation ^b	
Ba/Bb	46.4	>80	1.1
Za/Zb	51.5	>80	1.5
Ba/Zb	49.7	>80	0.9

^aConditions: 5.0 μM DNA, 100 mM NaCl, 10 mM phosphate buffer (pH 7.0), 20 $^\circ\text{C}$. ^bUV light at 340 nm was irradiated for 30 (**Ba/Zb**), 60 (**Ba/Bb**) or 120 min (**Za/Zb**). T_m of native duplex without stilbazole was 38.2 $^\circ\text{C}$. ^cObserved rate constant determined from initial slope of Figure 9.

was 46.4 $^\circ\text{C}$ (Figure 7a and Table 1), which was 8.2 $^\circ\text{C}$ higher than that of a native duplex without B residues (38.2 $^\circ\text{C}$). The T_m increased to more than 80 $^\circ\text{C}$ after photoirradiation. Thus, thermal stability of duplex was dramatically improved through photodimerization of the *p*-stilbazole moieties. The overall structure of photo-cross-linked duplex was analyzed by CD spectroscopy (Figure 7b). Before photoirradiation, positive exciton couplet was observed at around 260 nm, showing that

natural nucleobases adopted B-form duplex. An induced CD was observed at 320 nm, indicating that the *p*-stilbazoles are located in the chiral environment of DNA duplex. This induced CD band disappeared upon light irradiation because $\pi-\pi^*$ absorption of *p*-stilbazole at 325 nm disappears upon photocycloaddition. In the cross-linked species, the CD couplet at 260 nm remained almost unchanged to that prior to irradiation. These results indicated that overall B-form double-helical structure remained intact in spite of nonplanar structure of photodimerized *p*-stilbazoles.²⁴

Effect of Positive Charge on Photo-Cross-Linking Properties. We then investigated photo-cross-linking of *p*-methylstilbazolium, a stilbazole derivative containing a positive charge (*Z* in Scheme 1). The UV-vis spectra of a duplex tethering these moieties, *Za/Zb*, are shown in Figure 8. Before

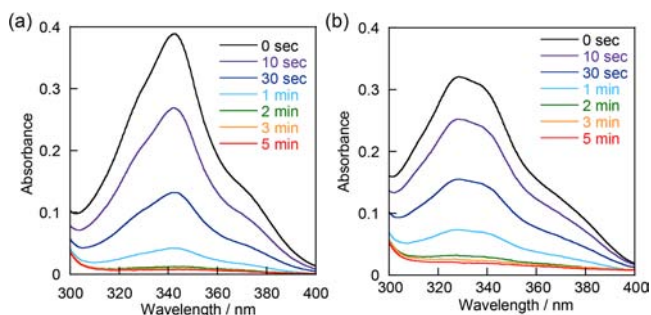


Figure 8. UV-vis spectra of (a) *Za/Zb* and (b) *Ba/Zb* before and after photoirradiation. Solution conditions were 5.0 μ M DNA, 100 mM NaCl, 10 mM phosphate buffer (pH 7.0), 0 $^{\circ}$ C.

photoirradiation, an absorption maximum was observed at 340 nm. This peak completely disappeared after photoirradiation for 3 min, unambiguously demonstrating that the photocycloaddition reaction between *Z* moieties occurred. The photo-cross-linking between *Z* moieties was further confirmed by HPLC and MALDI-TOF MS analyses (Figure S6). The T_m of *Za/Zb* before photoirradiation was 51.5 $^{\circ}$ C (Table 1 and Figure S7), about 5.1 $^{\circ}$ C higher than that of *Ba/Bb* (46.4 $^{\circ}$ C). The high stability of the *Z-Z* pair is due to electrostatic interactions between phosphate anions and cations of *Z* residues as we reported previously.²² In addition, cation- π interaction should also contribute to the high stability. The T_m of the *Za/Zb* increased to over 80 $^{\circ}$ C after photoirradiation at 340 nm, demonstrating significant stabilization upon photo-cross-linking of the *Z-Z* pair. We also investigated photocycloaddition of the hetero combination between *B* and *Z* residues (Figure 8b). Absorption maxima of *B* and *Z* residues at about 320 and 350 nm, respectively, simultaneously decreased upon irradiation. Thus, the *B-Z* pair can be photo-cross-linked in the context of DNA duplexes.

The observed rate constant of the reaction between *p*-methylstilbazolium residues was also determined from UV-vis spectra (Table 1 and Figure 9). The observed rate constants measured under the conditions of the same absorbance and light intensity are a measure of the relative quantum yields of reaction.³⁷ The observed rate constant of *Za/Zb* was 1.5 min^{-1} , which was almost the same order as that of the *p*-stilbazole duplex (1.1 min^{-1}).³⁸ The observed rate constant of hetero *B-Z* pair was also similar (0.9 min^{-1}). Thus, the cationic charge on the *Z* moiety did not significantly affect photoreactivity. In photodimerization reactions of *p*-stilbazole and *p*-methylstilbazolium not conjugated with DNA, the positive charge played

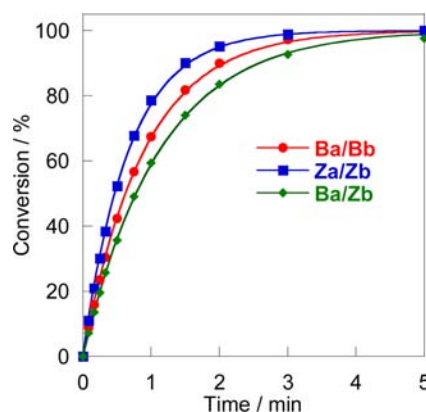


Figure 9. Reaction kinetics of *Ba/Bb* (red line), *Za/Zb* (blue line), and *Ba/Zb* (green line) determined from UV-vis spectra. Absorbances of all duplexes were adjusted to be almost the same (*Ba/Bb*: 0.186, *Ba/Zb*: 0.196, *Za/Zb*: 0.187).

important roles in both yield and stereoselectivity.^{24,39} Although the positive charge does affect the association process of stilbazoles, the “intrinsic” reactivity should be almost the same between *p*-stilbazole and *p*-methylstilbazolium. In other words, intrinsic photoreactivity of molecules can be evaluated by using DNA as a scaffold. Use of a DNA scaffold also allows reactivity of hetero combinations to be investigated while excluding the corresponding homo combinations.

Orthogonality with Natural Nucleobases. In order to serve as artificial base pairs, orthogonality is one of the most important prerequisites. Thus, we investigated orthogonality of *B-B* or *Z-Z* pairs with natural base pairs. Melting temperatures of *Xa/Xb* duplexes (where *X* was A, T, G, C, *B*, or *Z*) before photoirradiation are shown in Table 2. The *B* residue more

Table 2. Orthogonality of *B* or *Z* Moiety with Natural Nucleobases before Photoirradiation

	$T_m/^{\circ}\text{C}^a$					
	Aa	Ta	Ga	Ca	Ba	Za
Ab	25.7	40.3	30.6	24.4	31.6	30.4
Tb	42.8	28.7	33.6	26.4	34.0	31.8
Gb	30.7	31.9	29.8	45.9	33.9	32.4
Cb	27.3	26.8	48.8	23.8	35.1	32.2
Bb	33.7	37.4	36.3	36.0	46.4	50.9
Zb	32.5	34.4	35.1	34.7	49.7	51.5

^aConditions: 5.0 μ M DNA, 100 mM NaCl, 10 mM phosphate buffer (pH 7.0), 20 $^{\circ}$ C.

strongly hybridizes when the complementary residue is *B* than when it is a natural nucleobase. For example, *Ba/Bb* had a T_m of 46.4 $^{\circ}$ C, whereas duplexes of *Ba* with *Ab*, *Tb*, *Gb*, and *Cb* had much lower T_m s (31.6, 34.0, 33.9, and 35.1 $^{\circ}$ C, respectively). These T_m s were also significantly lower than those of duplexes with natural A-T or G-C pairs: The T_m of *Aa/Tb* (42.8 $^{\circ}$ C) was much higher than that of *Ab/Bb* (33.7 $^{\circ}$ C). The same tendency was observed with *Z-Z* pairs (Table 2). These results clearly demonstrated that *B-B* and *Z-Z* pairs show excellent orthogonality with natural nucleobases. In other words, the *B-B* or *Z-Z* pair could be used as “third base pair” for construction of DNA-based nanomaterials. The instability of a natural base paired with either *B* or *Z* is attributable to the sizes of the *B* and *Z* moieties; these stilbazoles are much larger than nucleobases, and intercalation of these moieties should

cause steric hindrance with D-ribose. In contrast, when B and Z moieties are paired, steric hindrance is likely lessened by flexible D-threoninol linkers. In addition, strong intermolecular stacking interactions between B and Z moieties should contribute to high stabilities of the duplexes containing two of these residues.

Next, orthogonality in the photo-cross-linking reaction was evaluated. When a B or Z moiety was located counter to A, T, G, or C, the UV-vis spectra did not change even after photoirradiation for 30 min (Figure S9).⁴⁰ Spectra of Ba/N (Figure 2b) and Za/N (Figure S10) did not change upon photoirradiation of the sample. This indicates that neither B nor Z react with natural nucleobases, whereas fast reactions occurred between B-B, Z-Z, and B-Z pairs. It has been reported that natural nucleobases, especially pyrimidine bases, may cause [2 + 2] photocycloaddition reactions. For example, a thymine dimer is formed upon UV irradiation that may induce point mutations.⁴¹ Photo-cross-linking agents, such as psoralen, form interstrand cross-link with thymine via photocycloaddition reactions.^{42,43} In our design, the vinyl group of *p*-stilbazole was located near the center of the natural base pair (Figure S11), but the reaction sites of nucleobases (e.g., C5 and C6 of pyrimidine bases) are toward the outside of the DNA duplex. Separation of vinyl group from pyrimidine inhibited cycloaddition reaction between *p*-stilbazole and natural nucleobases.

CONCLUSIONS

In conclusion, we have successfully developed artificial base pairs that can be photo-cross-linked in the context of a DNA duplex. When a duplex with a pair of *p*-stilbazoles located on opposite strands was irradiated with UV light, a [2 + 2] photocycloaddition reaction occurred significantly stabilizing the duplex. Both UV-vis spectra and HPLC analyses revealed that photo-cross-linking reaction was complete within 3 min. NMR analyses indicated that two diastereomers are produced on photo-cross-linking due to rotation of vinyl group. We have also demonstrated that *p*-stilbazole and *p*-methylstilbazolium showed high orthogonality with natural nucleobases in terms of both stability and photo-cross-linking reaction.

DNA has recently been used for construction of nanomaterials, such as nanoarchitecture and devices. However, the two natural base pairs, A-T and G-C, are not necessarily optimal in these materials. Furthermore, it is not necessary to mimic natural nucleobases when DNA is chemically synthesized and used as materials. The high stability and superb orthogonality of artificial base pairs of stilbazoles make them candidates for use in DNA nanomaterials. The photo-cross-linking reaction contributes remarkable stability to the DNA duplex. We believe that these pairs should be added to the “genetic alphabet” of DNA-based nanomaterials.

ASSOCIATED CONTENT

Supporting Information

Synthetic routes of *p*-stilbazole monophosphate, UV-vis, NMR, HPLC charts of duplexes tethering *p*-stilbazole and *p*-methylstilbazolium, energy-minimized structures are available. These materials are available free of charge via the Internet at <http://pubs.acs.org>.

AUTHOR INFORMATION

Corresponding Author

kashida@nubio.nagoya-u.ac.jp; asanuma@nubio.nagoya-u.ac.jp

Notes

The authors declare no competing financial interest.

ACKNOWLEDGMENTS

This work was supported by a Grant-in-Aid for Scientific Research (A) (21241031) and a Grant-in-Aid for Scientific Research on Innovative Areas “Molecular Robotics” (no. 24104005) from the Ministry of Education, Culture, Sports, Science and Technology, Japan. Partial support by The Asahi Glass Foundation (for H.A.) is also acknowledged.

REFERENCES

- (1) Krishnan, Y.; Simmel, F. C. *Angew. Chem., Int. Ed.* **2011**, *50*, 3124.
- (2) Seeman, N. C. *Annu. Rev. Biochem.* **2010**, *79*, 65.
- (3) Rajendran, A.; Endo, M.; Katsuda, Y.; Hidaka, K.; Sugiyama, H. *J. Am. Chem. Soc.* **2011**, *133*, 14488.
- (4) Meisenheimer, K. M.; Koch, T. H. *Crit. Rev. Biochem. Mol. Biol.* **1997**, *32*, 101.
- (5) Noll, D. M.; Mason, T. M.; Miller, P. S. *Chem. Rev.* **2005**, *106*, 277.
- (6) Cai, J.; Li, X.; Taylor, J. S. *Org. Lett.* **2005**, *7*, 751.
- (7) Lewis, R. J.; Hanawalt, P. C. *Nature* **1982**, *298*, 393.
- (8) Lewis, F. D.; Wu, T.; Burch, E. L.; Bassani, D. M.; Yang, J.-S.; Schneider, S.; Jaeger, W.; Letsinger, R. L. *J. Am. Chem. Soc.* **1995**, *117*, 8785.
- (9) Fujimoto, K.; Matsuda, S.; Takahashi, N.; Saito, I. *J. Am. Chem. Soc.* **2000**, *122*, 5646.
- (10) Ogino, M.; Fujimoto, K. *Angew. Chem., Int. Ed.* **2006**, *45*, 7223.
- (11) Ogasawara, S.; Fujimoto, K. *Angew. Chem., Int. Ed.* **2006**, *45*, 4512.
- (12) Ogasawara, S.; Ami, T.; Fujimoto, K. *J. Am. Chem. Soc.* **2008**, *130*, 10050.
- (13) Fujimoto, K.; Konishi-Hiratsuka, K.; Sakamoto, T.; Yoshimura, Y. *ChemBioChem* **2010**, *11*, 1661.
- (14) Tagawa, M.; Shohda, K.; Fujimoto, K.; Sugawara, T.; Suyama, A. *Nucleic Acids Res.* **2007**, *35*, e140.
- (15) Ihara, T.; Fujii, T.; Mukae, M.; Kitamura, Y.; Jyo, A. *J. Am. Chem. Soc.* **2004**, *126*, 8880.
- (16) Manchester, J.; Bassani, D. M.; Duprey, J.-L. H. A.; Giordano, L.; Vyle, J. S.; Zhao, Z.-y.; Tucker, J. H. R. *J. Am. Chem. Soc.* **2012**, *134*, 10791.
- (17) Mukae, M.; Ihara, T.; Tabara, M.; Jyo, A. *Org. Biomol. Chem.* **2009**, *7*, 1349.
- (18) Pasternak, K.; Pasternak, A.; Gupta, P.; Veedu, R. N.; Wengel, J. *Bioorg. Med. Chem.* **2011**, *19*, 7407.
- (19) Artificial base pairs, which can be synthesized enzymatically, have been reported by several groups. (a) Malyshev, D. A.; Dhami, K.; Quach, H. T.; Lavergne, T.; Ordoukhanian, P.; Torkamani, A.; Romesberg, F. E. *Proc. Natl. Acad. Sci. U.S.A.* **2012**, *109*, 12005. (b) Yang, Z.; Chen, F.; Alvarado, J. B.; Benner, S. A. *J. Am. Chem. Soc.* **2011**, *133*, 15105. (c) Kimoto, M.; Kawai, R.; Mitsui, T.; Yokoyama, S.; Hirao, I. *Nucleic Acids Res.* **2009**, *37*, e14. (d) Kaul, C.; Müller, M.; Wagner, M.; Schneider, S.; Carell, T. *Nat. Chem.* **2011**, *3*, 794.
- (20) Kashida, H.; Fujii, T.; Asanuma, H. *Org. Biomol. Chem.* **2008**, *6*, 2892.
- (21) Fujii, T.; Kashida, H.; Asanuma, H. *Chem.—Eur. J.* **2009**, *15*, 10092.
- (22) Kashida, H.; Ito, H.; Fujii, T.; Hayashi, T.; Asanuma, H. *J. Am. Chem. Soc.* **2009**, *131*, 9928.
- (23) Kashida, H.; Hayashi, T.; Fujii, T.; Asanuma, H. *Chem.—Eur. J.* **2011**, *17*, 2614.
- (24) Yamada, S.; Nojiri, Y.; Sugawara, M. *Tetrahedron Lett.* **2010**, *51*, 2533.
- (25) Quina, F. H.; Whitten, D. G. *J. Am. Chem. Soc.* **1977**, *99*, 877.
- (26) Yamada, S.; Uematsu, N.; Yamashita, K. *J. Am. Chem. Soc.* **2007**, *129*, 12100.
- (27) Liu, M.; Mao, X.-a.; Ye, C.; Huang, H.; Nicholson, J. K.; Lindon, J. C. *J. Magn. Reson.* **1998**, *132*, 125.

(28) Daku, L. M. L.; Linares, J.; Boillot, M.-L. *Phys. Chem. Chem. Phys.* **2010**, *12*, 6107.

(29) Turanova, O. A.; Gafiyatullin, L. G.; Gnezdilov, O. I.; Turanov, A. N. *Russ. J. Gen. Chem.* **2011**, *81*, 937.

(30) Liang, X. G.; Asanuma, H.; Kashida, H.; Takasu, A.; Sakamoto, T.; Kawai, G.; Komiyama, M. *J. Am. Chem. Soc.* **2003**, *125*, 16408.

(31) Bandara, H. M. D.; Burdette, S. C. *Chem. Soc. Rev.* **2012**, *41*, 1809.

(32) Gegiou, D.; Muszkat, K. A.; Fischer, E. J. *Am. Chem. Soc.* **1968**, *90*, 12.

(33) Here, we did not introduce spacers at the counter positions of *p*-stilbazole because incorporation of spacers rather destabilize duplex. See ref 20.

(34) B residues should be stacked in antiparallel manner in DNA. See also ref 21.

(35) Because peaks of *p*-stilbazole in *cis* form were not observed, all the *p*-stilbazole took *trans* form in DNA.

(36) On the other hand, only single peak was observed with **Ba/Bb** after photoirradiation as shown in Figure 4. Longer DNA portion of **Ba/Bb** would lessen the effect of structural difference of diastereomers compared with **Bc/Bd**.

(37) It is known that rate constant of photoreaction is affected by light intensity, absorbance, and quantum yield. Here, absorbances of **Ba/Bb**, **Ba/Zb**, and **Za/Zb** were adjusted to about 0.19. In addition, reaction kinetics of all duplexes was measured within several hours to avoid change of light intensity during the experiments. As a result, initial slope of Figure 9 (observed rate constant in Table 1) should be proportional to quantum yields.

(38) We also investigated effects of flanking sequence and mismatch on reaction rate constant of **B-B** combination. As a result, flanking AT pairs strongly facilitated photocrosslinking of *p*-stilbazole. Incorporation of mismatches decreased the rate constant. See Figure S8 for actual data.

(39) Takagi, K.; Suddaby, B. R.; Vadas, S. L.; Backer, C. A.; Whitten, D. G. *J. Am. Chem. Soc.* **1986**, *108*, 7865.

(40) Although absorbance of *p*-stilbazole (**B** residue) slightly decreased probably due to photodegradation, the reaction was much slower than photocrosslinking reaction.

(41) Lukin, M.; de los Santos, C. *Chem. Rev.* **2006**, *106*, 607.

(42) Hearst, J. E. *Annu. Rev. Biophys. Bioeng.* **1981**, *10*, 69.

(43) Lee, B. L.; Murakami, A.; Blake, K. R.; Lin, S. B.; Miller, P. S. *Biochemistry* **1988**, *27*, 3197.